

Symbiont shuffling induces differential DNA methylation responses to thermal stress in the coral *Montastraea cavernosa*

Javier A. Rodriguez-Casariego¹  | Ross Cunning^{2,3}  | Andrew C. Baker³ |
Jose M. Eirin-Lopez¹ 

¹Environmental Epigenetics Laboratory, Institute of Environment, Florida International University, Miami, Florida, USA

²Daniel P. Haerther Center for Conservation and Research, John G. Shedd Aquarium, Chicago, Illinois, USA

³Department of Marine Biology and Ecology, Rosenstiel School of Marine and Atmospheric Science, University of Miami, Miami, Florida, USA

Correspondence
Jose M. Eirin-Lopez, Environmental Epigenetics Laboratory, Florida International University, North Miami, Florida, USA.
Email: jeirinlo@fiu.edu

Funding information
National Oceanic and Atmospheric Administration, Grant/Award Number: NA21NMF4820301; Mote Marine Laboratory and Aquarium, Grant/Award Number: POR2016-15; National Science Foundation, Grant/Award Number: 1547798 and 1921402

Abstract

Algal symbiont shuffling in favour of more thermotolerant species has been shown to enhance coral resistance to heat-stress. Yet, the mechanistic underpinnings and long-term implications of these changes are poorly understood. This work studied the modifications in coral DNA methylation, an epigenetic mechanism involved in coral acclimatization, in response to symbiont manipulation and subsequent heat stress exposure. Symbiont composition was manipulated in the great star coral *Montastraea cavernosa* through controlled thermal bleaching and recovery, producing paired ramets of three genets dominated by either their native symbionts (genus *Cladocopium*) or the thermotolerant species (*Durusdinum trenchii*). Single-base genome-wide analyses showed significant modifications in DNA methylation concentrated in intergenic regions, introns and transposable elements. Remarkably, DNA methylation changes in response to heat stress were dependent on the dominant symbiont, with twice as many differentially methylated regions found in heat-stressed corals hosting different symbionts (*Cladocopium* vs. *D. trenchii*) compared to all other comparisons. Interestingly, while differential gene body methylation was not correlated with gene expression, an enrichment in differentially methylated regions was evident in repetitive genome regions. Overall, these results suggest that changes in algal symbionts favouring heat tolerant associations are accompanied by changes in DNA methylation in the coral host. The implications of these results for coral adaptation, along with future avenues of research based on current knowledge gaps, are discussed in the present work.

KEY WORDS

coral bleaching, *Durusdinum*, epigenetics, great star coral, MBD-BS, symbiont shuffling, thermotolerance

1 | INTRODUCTION

The obligate symbiosis between corals and dinoflagellates in the family Symbiodinaceae constitutes one of the most successful biological strategies supporting remarkable biodiversity in very oligotrophic waters. This highly efficient symbiosis, however, is sensitive to elevated temperatures, among other stressors, leading to the

disruption of the partnership in a stress response known as "coral bleaching" (Baker & Cunning, 2015; Weis, 2008), often resulting in mortality. Bleaching is the main cause of the accelerated decline of coral populations, mainly caused by the anthropogenic alteration of the planet's climate (Hughes et al., 2017; Pandolfi et al., 2003), with dire consequences for marine ecosystems and coastal populations. Hence, great efforts have been placed in understanding the

dynamics and the mechanisms regulating this symbiosis as a way to develop strategies to increase coral resilience to global change (Bay et al., 2019; National Academies of Sciences, Engineering, & Medicine et al., 2019).

Several factors have been shown to modulate coral sensitivity to heat stress and promote acclimation/adaptation responses (i.e., genetic, epigenetic, symbiotic community composition and microbiome [Barshis, 2015; Eirin-Lopez & Putnam, 2019; Quigley et al., 2018]), leading to a wide spectrum of bleaching susceptibility patterns. Focusing on the symbiotic relationship, both the identity and population density of the symbiont appear to affect thermal sensitivity (Baker, 2004; Cunning & Baker, 2013; Silverstein et al., 2015; Swain et al., 2020). Particularly, corals hosting symbionts in the genus *Durusdinium* often display higher tolerances to heat stress (Berkelmans & van Oppen, 2006; Silverstein et al., 2015) and improved overall survival to bleaching events (Glynn et al., 2001; Jones et al., 2008). Current evidence of an increase and persistence of *Durusdinium* in natural coral populations, with a recent and rapid expansion through the Caribbean (Pettay et al., 2015), suggests a positive selection of this symbiotic partner under increasingly frequent thermal anomalies. Consequently, increasing efforts have been placed to study the mechanisms underlying coral symbiotic interactions under stress conditions (Cunning & Baker, 2020; Helmkampf et al., 2019; Yuyama et al., 2018). Yet, with the exception of a single study investigating the epigenetic regulation of transcriptional changes upon the establishment of symbiosis (Li et al., 2018), the role of epigenetic mechanisms regulating molecular responses to changes in coral symbiont composition under thermal stress remains unknown.

Accumulating evidence suggests that epigenetic modifications (i.e., molecules and mechanisms able to regulate gene expression through the generation of alternative gene activity states in the context of the same DNA sequence [Cavalli & Heard, 2019]) are involved in modulating genomic responses to environmental signals conveyed to the genome through signal transduction pathways, and thus participating in the regulation of subsequent phenotypic responses. Epigenetic regulation is ubiquitous in all eukaryotes, based on the fundamental role that epigenetic mechanisms play in genome packing and functional organization within the cell nucleus. In corals, several studies have already reported evidence of epigenetic responses to different types of environmental stressors such as thermal stress, ocean acidification, and eutrophication, among others (Putnam et al., 2016; Liew et al., 2018; Dimond et al., 2017; Putnam et al., 2016; Liew et al., 2018; Rodriguez-Casariego et al., 2018), as well as to broad environmental change (Rodríguez-Casariego et al., 2020; Dimond & Roberts, 2020; Durante et al., 2019; Liew et al., 2020), with links to transcriptional plasticity (Dixon et al., 2018; Li et al., 2018). Since the symbiotic partners of corals also constitute part of (and therefore shape) their environment, the present work hypothesizes that transitions in these populations will require phenotypic acclimatory responses in the coral host, facilitated by epigenetic modifications. Indeed, coral symbiont variants and abundance have

been shown to significantly modulate gene expression in the host (Barfield et al., 2018; Helmkampf et al., 2019), including experiments where the intergenet variability (genet refers to the collection of fragments or "ramets" originating from the same colony [Cunning & Baker, 2020; DeSalvo et al., 2010]) was eliminated. Moreover, in the cnidarian model *Aiptasia*, Li et al. (2018) evidenced the role of epigenetic mechanisms modulating transcriptional changes during the establishment of symbiosis. In order to elucidate the role of epigenetic regulation during symbiont transitions in corals, the present work builds on the experimental design developed by Cunning and Baker (2020) in which symbionts were manipulated to produce paired ramets with different symbionts to subsequently expose them to thermal stress. Epigenetic changes in DNA methylation occurring in response to symbiont manipulation and subsequent thermal stress exposure are examined, as well as their relationship with gene expression. The obtained results suggest that DNA methylation response to thermal stress is symbiont species-specific, with differentially methylated sites occurring more often in repetitive regions of the genome. Evidence of gene-body methylation reducing spurious transcription was obtained, but not mediating changes in gene expression.

2 | MATERIALS AND METHODS

2.1 | Experimental design

Detailed description of coral collection, fragmentation, and subsequent symbiont manipulation and short-term thermal stress exposure can be found in (Cunning & Baker, 2020). Briefly, wild colonies of the great star coral *Montastraea cavernosa* were collected near Key Biscayne, FL, fragmented by coring into 2.5 cm diameter ramets, and acclimated to the University of Miami's Marine Technology and Life Sciences Seawater Complex water systems for 3.5 months (26°C, ~230 μmol photons $\text{m}^{-2} \text{s}^{-1}$ in a 12-hr:12-hr light-dark cycle, fed Reef Chili twice a week). After this period, half of the ramets were maintained in control conditions while the other half were subjected to controlled bleaching (temperature was raised from 26 to 32°C at 0.5°C day 1, and kept at 32°C for 14 days) and recovery (fragments were transferred to control conditions at 26°C), which encouraged symbiont community changes in favour of *Durusdinium*. After a 4-month recovery period, coral symbiotic composition was assessed through qPCR (Cunning & Baker, 2013), confirming symbiont shuffling from *Cladocopium* to *Durusdinium* dominance. Paired (same coral genotype) *Cladocopium*- and *Durusdinium*-dominated ramets were then exposed to control (26°C) or short-term heat-stress conditions for 4.8 days (~3 degree heating weeks, DHWs) and subsequently flash frozen in liquid nitrogen for long-term preservation of samples. Manipulations resulted in four groups, control corals hosting *Cladocopium* (C_C), control corals hosting *Durusdinium* (D_C), heat-stressed corals hosting *Cladocopium* (C_H) and heat-stressed corals hosting *Durusdinium* (D_H).

2.2 | Coral DNA extraction and MBD-BS library preparation

In the present study, DNA methylation was studied using a Methyl-binding domain capture approach coupled with bisulphite sequencing (MBD-BS). This method allows the enrichment of methylated DNA (as low as 1% of the genome in some invertebrates) to reduce sequencing requirements, while maintaining base-pair resolution of the resulting data. From the subset of flash-frozen samples (see above), a total of $n = 2$ replicates per genotype, $n = 3$ genotypes, for all four symbiont/temperature combinations were randomly selected for methylation analyses ($n = 24$ samples). Genomic DNA was isolated from flash frozen coral cores after pulverization in liquid nitrogen. Approximately 100 mg of the resulting powder was resuspended in 2 ml vials containing 500 mg of Zirconia/Silica beads (0.5 mm diameter) and 1 ml of DNA/RNA Shield buffer (Zymo Research). Coral cells were gently lysed with two 30 s vortex pulses to enrich host DNA by maintaining symbiont cells intact (Rodríguez-Casariego et al., 2020). After centrifugation (12,000 $\times g$ for 5 min), 800 μ l of the supernatant were transferred to a new tube and DNA isolation was continued using the Quick-DNA/RNA Mini-Prep kit (Zymo Research) as per the manufacturer's instructions. DNA quality was assessed by gel electrophoresis and spectrophotometric analysis as described in our previous work (Rivera-Casas et al., 2017). DNA concentration was measured using a Qubit 2.0 fluorometer (Thermo Fisher). Samples with concentrations under 20 ng/ μ l and/or low quality (i.e., ethanol contamination) were re-processed using a DNA Clean & Concentrator kit (Zymo Research, Irvine, CA) until proper concentration and quality were achieved.

DNA samples ranging from 36.2 to 119 ng/ μ l (100 μ l) were placed in 1.5 ml polystyrene tubes and sheared in a Bioruptor (Diagenode) using 25 cycles of 30 s ON and 30 s OFF in low power. Shearing size (~350 bp) was confirmed using a 2100 Bioanalyser with high sensitivity DNA assay kit (Agilent Technologies). Capture of methylated DNA was performed with the MethylCap Kit (Diagenode). A single-fraction elution was performed with 150 μ l of high-salt buffer to obtain captured DNA only. Purification of the captured DNA was performed with the DNA Clean & Concentrator kit (Zymo Research), and eluted in 25 μ l. Bisulphite conversion and library preparation was performed using the Pico Methyl-Seq Library Prep Kit (Zymo Research). Libraries were barcoded and shipped for pooling and sequencing at Admera Health Biopharma Services, generating 150 bp paired-end reads on two lanes of a HiSeq-X sequencer.

2.3 | DNA methylation quantification

Sequences were trimmed with 10 bp removed from both the 5' and 3' ends using TrimGalore! v.0.4.5 (Krueger, 2012). Sequence quality was assessed using FastQC v.0.11.7 (Andrews, 2010) before and after trimming. The *M. cavernosa* genome assembly (July 2018 version) was obtained from Dr. M. Matz's Laboratory (<https://matzlab.weebly.com/data--code.html>). This assembly was constructed

with a combination of PacBio and 10x Genomics reads, resulting in a genome size of 448 Mb, similar to other scleractinian genomes (Shinzato et al., 2011; Prada et al., 2016; Voolstra et al., 2017). In terms of quality, the assembly has 5161 contigs with a maximum length of 1872.9 kb, an N50 of 343 kb and a 65.5% completeness (BUSCO, C:65.5% [S:63.4%, D:2.1%, F:5.5%, M:29.0%]). This quality is much lower than more recent assemblies (Shinzato et al., 2021) but is comparable with the first *A. digitifera* assembly (Shinzato et al., 2011). For methylation analysis the genome was prepared for downstream use with the Bismark genome_preparation function (Bismark v.0.19.0, Krueger & Andrews, 2011) using Bowtie 2-2.3.4 (Langmead & Salzberg, 2012) as aligner. Trimmed sequences were then aligned to the prepared genome using Bismark with nondirectionality and alignment score of L,0,-1.2. Alignment files (i.e.,.bam) were deduplicated (using deduplicate_bismark), sorted and indexed (using SAMtools v.1.9 [Li et al., 2009]). Methylation calls were extracted from deduplicated files using bismark_methylation_extractor and separated by context (i.e., CpG, CHG, CHH).

Genomic feature tracks for downstream analyses were derived directly from the *M. cavernosa* genome annotation (<https://matzlab.weebly.com/data--code.html>) or created using BEDtools v2.26.0 (Quinlan & Hall, 2010). Genes, mRNA, exons, coding sequences (CDS), and flanking untranslated regions (3'-UTR and 5'-UTR) were obtained directly from the genome annotation file while putative promoter regions, intergenic regions and repetitive regions were created following previously developed pipelines (Venkataraman et al., 2020; see data availability for access to the modified code). Introns were derived by subtracting exons from gene tracks. Gene body methylation includes CpGs overlapping with intron, CDS and UTRs, but not promoters.

2.4 | Statistical analyses

Statistical analyses were all completed in R (v4.0.2; R Core Team, 2020) with RStudio (v1.3.959; R Studio Team, 2020). R scripts used for all analysis were stored in Github (see data availability statement).

2.4.1 | Describing the DNA methylation landscape

Sequences from all samples were used to characterize general DNA methylation patterns in *M. cavernosa*. Methylation calls per CpG loci (i.e., cov files) were merged, corrected using a 1% miss-call rate (based on non CpG methylation calls) and filtered to maintain individual CpG dinucleotides with at least 5x coverage in each sample. Individual loci (i.e., CpG dinucleotides) were classified based on methylation percent in unmethylated (<10% methylation), sparsely methylated (10%–50% methylation) and methylated (>50% methylation). The genomic features loci overlap with were also characterized (i.e., CDS, intron, UTRs, putative promoters, transposable elements and other intergenic regions). The significant association between genomic features and methylation status was evaluated through a

chi-squared test (prop.test R function) using a CpG track extracted from the genome assembly. A similar approach was followed for the feature overlap of differentially methylated regions (DMR).

2.4.2 | Genome-wide DNA methylation response

The genome-wide DNA methylation response (all CpG loci) induced by the experimental manipulation (symbiont and temperature) was visualized through principal coordinates analysis (PCoA) of Manhattan distances. A variance partitioning analysis was performed using the R package *variancepartition* (Hoffman & Schadt, 2016), to visualize the variance components within each coral genet. Treatment associated variance across all genets was analysed through a discriminant analysis of principal components (DAPC) using the R package *adegenet* v2.1.3 (Jombart et al., 2010). The effect of experimental manipulations in Global percent DNA methylation was also tested by ANOVA with the model *aov(median~Treatment*Symb*feature)*.

2.4.3 | Describing DNA methylation in repetitive regions

Repetitive regions in *M. cavernosa* were annotated using RepeatMasker v4.1.1 (Smit et al., (20??) RepeatMasker at <http://repeatmasker.org>). Python scripts developed by Dr. Yi Jin Liew were used to calculate methylation levels (average % methylation for all sites overlapping repeats: https://github.com/lyijin/smic_dna_meth/blob/master/descriptive_wgbs/overlap_rep_elements/check_meth_level_in_repeats.per_type.py) and methylation densities (number of methylated Cs: https://github.com/lyijin/smic_dna_meth/blob/master/descriptive_wgbs/overlap_rep_elements/check_meth_density_in_repeats.per_type.py) per repeat type. The significance of the effect of the treatment combinations over DNA methylation density on repeats was evaluated through a two-way ANOVA and pairwise *t* test.

2.4.4 | Determining expression of repetitive elements

The expression of transcripts originating from repeat elements was quantified utilizing the RNA-seq data set developed by (Cunning & Baker, 2020; NCBI Accession no. PRJNA610282). Reads from each sample included in the methylation analysis ($n = 24$) were mapped against the genome of *M. cavernosa* with HISAT2 v2.1.0 (Kim et al., 2015). The resulting aligned reads (between 75% and 90% mapping efficiency) were processed using samtools depth (Li et al., 2009) to create a per-base coverage file. RNA-seq reads counts for each repeat type were parsed utilizing a python script developed by Dr. Yi Jin Liew (https://github.com/lyijin/smic_dna_meth/blob/master/descriptive_rnaseq/overlap_rep_elements/check_expr_in_repeats.per_type.py).

The significance of the effect of experimental manipulations on the expression of repetitive regions was evaluated through paired *t* tests.

2.4.5 | Identification of differentially methylated regions and genes

Differentially methylated regions (DMRs) were identified using the methylpy pipeline (Schultz et al., 2015) (<https://github.com/shellytrigg/methylpy>). This method first identifies differentially methylated CpGs between all samples using a mean square root test, and then collapses neighboring sites across a specific window size. CpG sites with at least 5x coverage were subject to DMR analysis across a 250 bp window. DMRs were identified from all samples together, and between relevant symbiont/temperature combinations. Regions with less than three CpGs and present in less than 75% of the samples in each treatment were discarded. Significant differences of DMRs between treatments was further tested through ANOVA after arcsine-square-root transformation. Two-way ANOVA with the model *~symbiont*temperature* was applied for DMRs identified from all samples together, and one-way ANOVA was employed for combination contrasts (i.e., C_H vs. C_C ; D_C vs. C_C , etc.).

Differentially methylated genes (DMG) were identified through a generalized linear model implemented in R. CpG methylation (>5x coverage) across gene-body (intron, CDS and UTRs) was summarized for each gene as the sum of all methylated and unmethylated reads for a particular position across the gene. The model *glm(meth, unmeth~sym*temp, family = binomial)* was applied to all samples, while models including only sym or temp were applied to individual combination contrasts as described before. Only positions shared by all samples were included in the analyses.

2.4.6 | Functional enrichment of methylated genes and association with gene expression

Gene ontology (GO) and eukaryotic orthologous groups (KOG) categories enrichment in relation to gene-level DNA methylation was performed using GO-MWU (Wright et al., 2015) and KOG-MWU (Matz, 2016) respectively. Methylation change between treatment contrasts used for both enrichment analyses was calculated as log2 fold of the methylated/unmethylated fraction per gene. *M. cavernosa* KOG and GO categories used here are the same as in (Cunning & Baker, 2020) and were obtained from Cunningham (2020: <https://doi.org/10.5281/zenodo.3895128>). Additional GO enrichment analysis, using topGO (Alexa et al., 2006), was performed to identify categories significantly overrepresented in DMGs. Similarities between the methylation responses of group contrasts were evaluated by correlation of KOG delta-ranks.

Gene expression data, as counts per sample/gene, was obtained from archived data sets (<https://doi.org/10.5281/zenodo.3895128>) associated with Cunningham and Baker (2020) and filtered to include

only the samples for which DNA methylation data was generated here. The correlation between these data sets was tested with linear regression, including gene-body methylation mean (methylated/unmethylated CpGs), gene expression mean (log2-cpm) and its respective coefficient of variance (methCV and expressionCV). Variable generation was based on code described in Downey-Wall et al. (2020).

3 | RESULTS

3.1 | The DNA methylation landscape of *M. cavernosa*

Sequencing of 24 MBD-captured bisulphite libraries resulted in a total of ~800 million paired-end 150 bp-long reads (NCBI accession no. PRJNA750791; Figure S1), among which ~779 million passed the quality filtering, and 192 million (deduplicated reads) mapped to the genome of *M. cavernosa*. Across all samples, 9,993,450 CpG sites (~36% of 28,118,748 CpGs in the genome) passed error filtration (1% miss-called Cs) and 8,412,240 (~30% of all CpGs in the genome) had at least 5x coverage. Although mapping and coverage varied between samples, the patterns were not treatment-specific (Figure S2).

All CpG sites, after error and coverage filtering, were used to characterize the general DNA methylation landscape (Figure 1). As expected from the enrichment caused by the MBD method, most of the CpGs covered by sequencing were either methylated (5,226,176; 62.1%) or sparsely methylated (2,881,642; 34.3%) with only 304,422 (3.6%) being unmethylated. The observed CpG-methylation level was dependent on genomic location ($p < .001$; Table S1), with introns and repetitive regions having proportionally higher methylated CpGs (>50% median methylation) compared to all CpGs in the genome (Figure 1a, Table S1). Methylated CpGs overlapped primarily

with intergenic regions (including repeats), with only ~30% overlapping with genic and flanking regions (Figure 1a). Introns and exons, however, showed higher methylation levels (%) than intergenic regions (Figure 1b).

3.2 | DNA methylation response to symbiont shuffling and heat stress

Only CpG positions with >5x coverage that were present in at least 80% of samples per treatment were used for evaluating epigenetic changes caused by symbiont manipulation and/or thermal stress. Principal coordinate analysis (Figure 2a) revealed that samples clustered primarily by genotype along the PC2 axis, with the effect of treatment groups somewhat evident across PC1, although the separation along this axis is not consistent between genotypes. Variance partitioning analysis (Figure 2b) also confirmed that the effects of the symbiont manipulation and heat stress were not homogeneous across genotypes, with the effects of symbiont manipulations and thermal exposure contributing differently among colonies. Across all genotypes, however, most of the variance was explained by the interaction between symbiont and temperature, indicating variable methylation responses to heat stress in corals hosting different symbionts. Significant differences in global methylation (calculated as median methylation of all CpGs) due to thermal stress ($F = 5.943, p = .0171$), but not to symbiont manipulation ($F = 0.572, p = .4519$) or its interaction with thermal stress ($F = 0.648, p = .4234$) were observed using a two-way ANOVA, indicating that methylation is mainly affected by thermal stress, which cannot be shown in PCoA and variance partitioning..

The discriminant analysis of principal components (Figure 2c for all CpGs; Figure S3 by feature) identified consistent differences in DNA methylation profiles corresponding to the experimental variables across genets. Along the first discriminant axis (LD1) corals

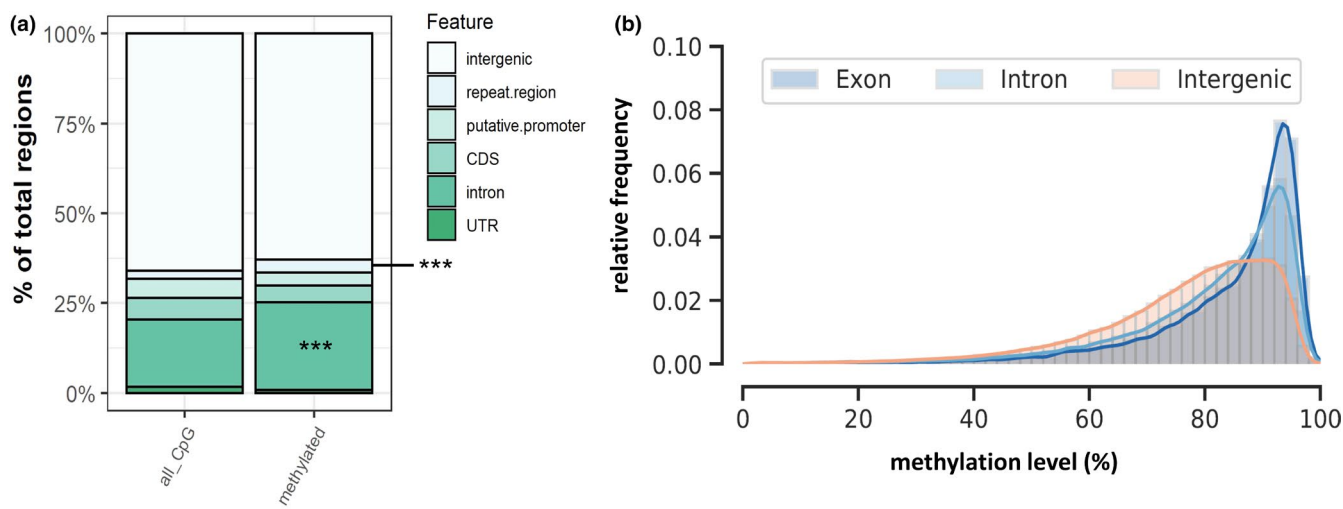


FIGURE 1 DNA methylation characteristics of *M. cavernosa*. (a) CpG overlap with genomic features: “all_CpG” refers to all positions in the genome of *M. cavernosa* regardless of their methylation status; “methylated” refers to CpG showing over 50% median methylation. Significant interaction between methylation and features was obtained (p -value $< 2.2e-16$). Significant proportional enrichment is represented with asterisks (** represents $p < .001$, see Table S1 for details). (b) Distribution of DNA methylation levels (% methylation) in exons, introns, and intergenic regions

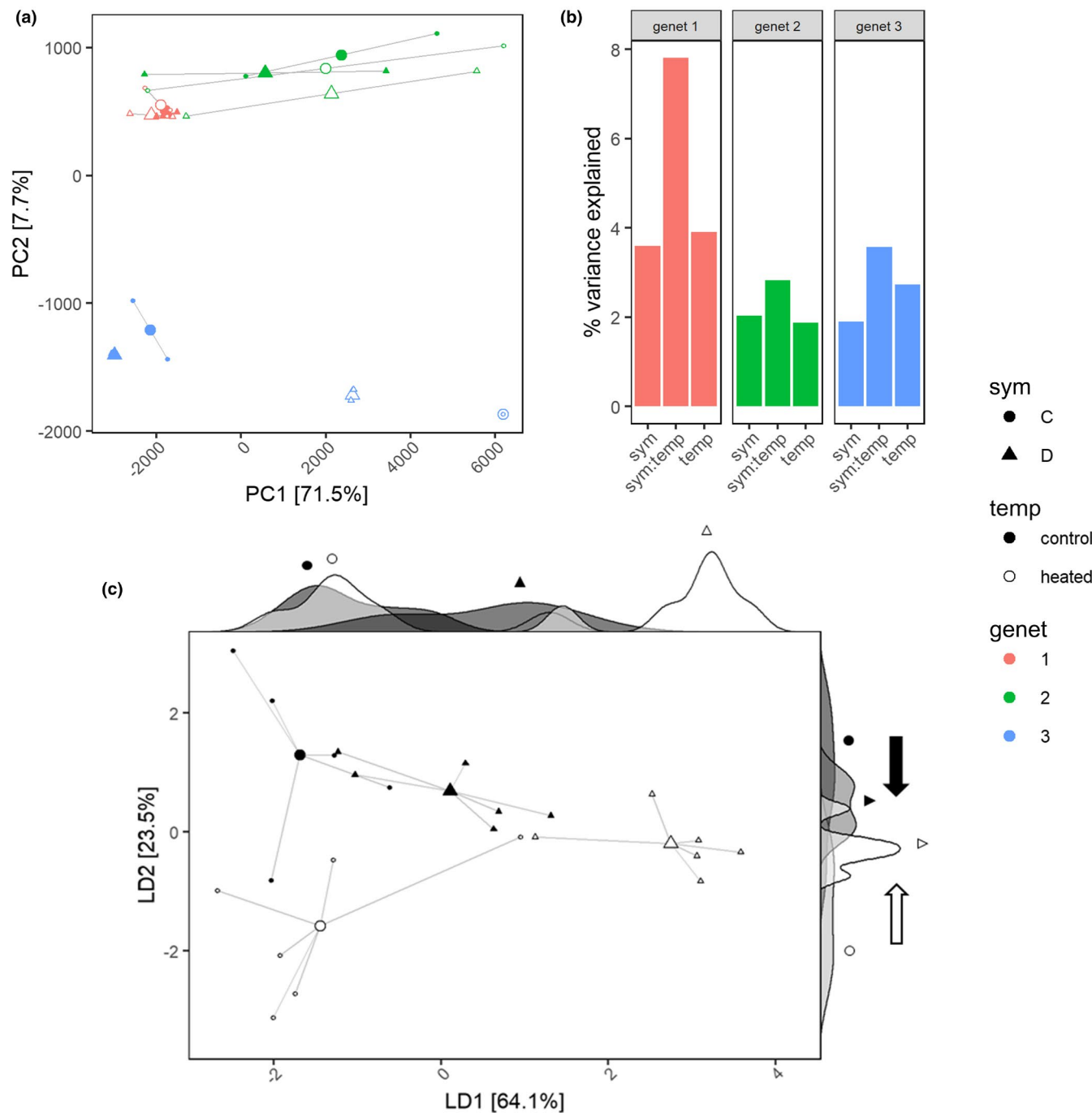


FIGURE 2 DNA methylation variation in *M. cavernosa* corals ($N = 3$ genets) manipulated to host different symbionts (sym) and then exposed to thermal stress (temp). (a) Principal coordinate analysis of percent DNA methylation at single CpGs (>5 x coverage) shared by all samples after variance-stabilization ($n = 22,953$ loci). (b) Sources of variance in DNA methylation calculated as a percentage of the total variance within each coral genet. (c) Discriminant analysis of principal components (DAPC) of single CpG methylation profiles. Density plots showing the distribution of samples across each discriminant function (LD1 and LD2) are shown across the top and left of the figure. Arrows illustrate the different position of corals dominated by *Durusdinium* symbionts compared with those dominated by *Cladocopium* of the same thermal treatment. C refers to native symbionts in the genus *Cladocopium* and D refers to manipulated symbionts (*D. trenchii*). Small symbols represent coral samples and larger symbols represent centroids of two replicates

hosting *Durusdinium*, towards the right, separate from those hosting *Cladocopium*, towards the left. Heat stress response was evident along the second discriminant function (LD2), with control

corals hosting *Durusdinium* separating from control corals hosting *Cladocopium* in the same direction of the heat stress response. Remarkably, *Durusdinium*-dominated corals exposed to thermal

stress move very little along LD2 but separate from control along LD1. The separation by dominant symbiont was larger in corals exposed to heat stress, denoting a divergent response dependent on the symbiont. This pattern of methylation in response to symbiont change, resembling the *Cladocopium*-dominated corals thermal response, as well as the different DNA methylation response to temperature in corals hosting *Durusdinium*, was also evident across genomic features such as gene bodies, introns, intergenic regions and transposable elements (Figure S3).

3.3 | Overlapping between differential DNA methylation and genomic features

Regional changes in DNA methylation are more likely to affect genomic functioning than variation in individual CpGs. Consequently, DMRs were identified by combining differentially methylated cytosines (*methylpy* pipeline) across 250 bp windows. DMRs (Table 1) were determined by either comparing samples from all four treatment combinations (*all*-DMR) or from each of the four individual treatment contrasts, such as symbiont shuffling under control temperature (D_C vs. C_C), heat stress response for both symbiont types (C_H vs. C_C , and D_H vs. D_C), and the combination of both symbiont manipulation and temperature (D_H vs. C_H). Across all-DMR comparison, symbiont manipulation produced the highest number of DMRs (80). This was mostly contributed by the D_H versus C_H contrast with almost 10 times the number of DMR's produced by the D_C versus C_C contrast (Table 1). Interestingly, *Cladocopium*-dominated corals heat-stress response involved almost three times more DMRs than that of *Durusdinium*-dominated, hinting a potential "milder" methylation response to heat-stress in corals hosting *Durusdinium*.

Heatmaps were used to illustrate methylation changes caused by symbiont manipulation and thermal exposure on significant DMRs (Figure 3a). Across all 206 unique significant DMRs identified from the four treatment contrasts (Figure 3a), five distinctive clusters (a to e) were defined. DMRs in cluster a show DNA methylation changes that are responsive to both symbiont and temperature, with a reduction in methylation from control-corals hosting *Cladocopium* to both heated-corals hosting the same symbiont and control corals hosting *Durusdinium*. DNA methylation response to temperature of

TABLE 1 Differentially methylated regions (DMRs) for general model output and across treatment contrasts

Contrast	All	sig_symb	sig_temp	sig_inter
<i>all</i> -DMRs	34,419	80	68	62
$D_C C_C$ -DMRs	15,598	15 (6, 9)		
$C_H C_C$ -DMRs	17,000		73 (30, 43)	
$D_H D_C$ -DMRs	18,353		26 (8, 18)	
$D_H C_H$ -DMRs	21,585	132 (73, 59)		

Total significant DMRs (hypermethylated, hypomethylated) are represented for contrasts.

corals hosting *Durusdinium* show an opposite direction than that of *Cladocopium* dominated corals in this cluster, confirming a different response to stress in corals dominated by each symbiont. Clusters b and d comprise DMRs responding exclusively to symbiont manipulation but with opposite directions of methylation change. DMRs in cluster c show a shared methylation response to temperature for corals hosting both symbionts. In cluster e, DMRs show little change between control corals hosting both symbionts, but the demethylation response to heat stress is smaller in corals hosting *Durusdinium*. Overall, DNA methylation seems to be responding differently to symbiont manipulation and heat stress, as evidenced in the small number of DMRs shared between treatments (Figure 3c) with some evidence of a milder response to temperature in corals dominated by *Durusdinium* symbionts.

Significant DMRs in all clusters mostly overlapped with intergenic regions, although gene bodies of 68 genes were represented (Table S2). DMRs in each cluster showed dependence on genomic regions. Intergenic regions were enriched in DMRs for cluster c, although not significantly (chi square $p < .1$), while repetitive regions were significantly overrepresented in cluster d (chi square $p < .0001$; Figure 3b). Intronic regions were overrepresented in cluster e, but this enrichment was not significant. These marked differences in DMRs localization also support a differential response to symbiont manipulation and thermal stress.

3.4 | DNA methylation and expression of repetitive regions

Given the observed prevalence of methylated positions across repetitive regions and the significant representation of these genomic elements in DMRs, a more detailed analysis of DNA methylation distribution and variation across these features was performed, as well as the evaluation of their expression. No significant change in global methylation density or expression was observed between treatment combinations when all repeat types were combined (Figure 4). However, significant changes in the expression of long terminal repeats (LTR; Figure 4b) were observed for both thermal stress contrasts (C_H vs. C_C (*t* test: $p = .0238$); D_H versus D_C (*t* test: $p = .0169$)). Although methylation density in these repeats showed a similar trend (Figure 4a), these changes were not significant. However, DMRs overlapping with repeats showed a significant proportional enrichment in LTR for both D_C versus C_C (*prop_test*: $p = .0360$) and D_H versus C_H (*prop_test*: $p < .0001$). Combined, these results are indicative that DNA methylation in repetitive regions is responsive to environmental change, and that transposable elements are activated under thermal stress.

3.5 | Gene body methylation and functional enrichment

Gene methylation information was obtained for 1040 genes represented across all groups and covered by at least 3 CpGs.

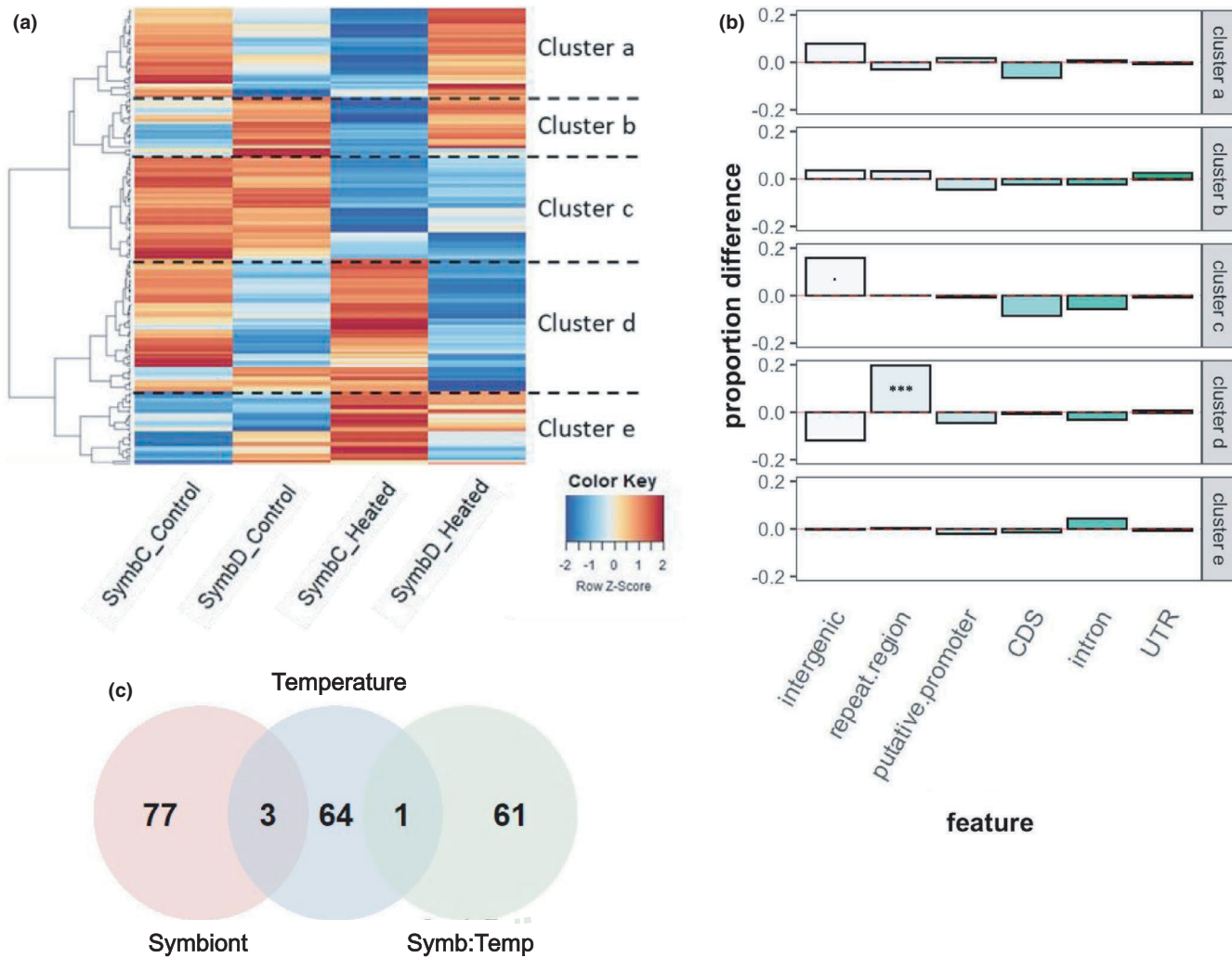


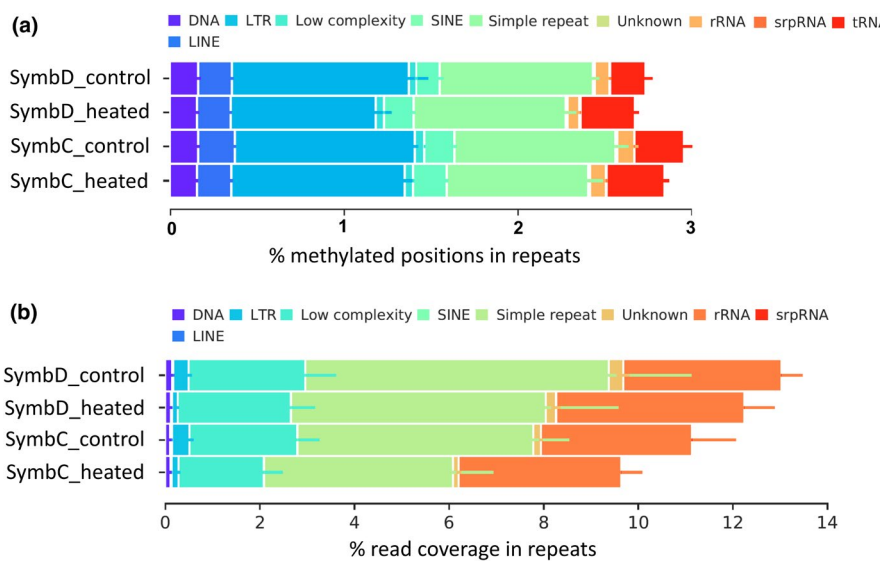
FIGURE 3 DNA methylation across differentially methylated regions (DMRs). (a) Heatmap of DNA methylation variation (as deviation from the mean; z-score) of significant DMRs for all experimental contrasts. Clusters represent groups of DMRs with similar patterns of methylation change. (b) Genomic features overlapping with DMRs and differences between proportions of CpGs overlapping with each feature within each DMR and through all the regions analyzed. Significance of a chi-square proportion test are represented for enriched regions ($\cdot = p.\text{adj} < .1$; $*$ $p.\text{adj} < .05$; $**p.\text{adj} < .001$; $***p.\text{adj} < .0001$). (c) Venn diagram illustrating shared DMRs between treatment comparisons

Differentially methylated genes (DMGs) were determined through a binomial generalized linear model with *symbiont type*, *temperature* and the interaction as levels, and also as 1v1 comparisons for the contrasts described before. Across all 430 DMGs obtained, there was a significant reduction in global DNA methylation between control and heated *Cladocopium*-dominated corals (t test, $p.\text{adj}_{\text{BH}} = .047$; Figure 5a) and a nonsignificant increase in control corals hosting *Durusdinium* when compared with *Cladocopium* dominated controls (t test, $p.\text{adj}_{\text{BH}} = .912$). There was also a slight reduction in global DNA methylation in response to temperature for *Durusdinium*-dominated corals, but it was not significant (t test, $p.\text{adj}_{\text{BH}} = .486$). The contrast D_{H} vs. C_{H} produced the largest number of DMGs (286, Figure 5d) while D_{H} vs. D_{C} produced less than half of all other contrasts (106 DMGs). Comparisons including different symbionts (D_{C} vs. C_{C} and D_{H} vs. C_{H}) shared 130 DMGs, while only 62 were shared between temperature contrasts for both symbionts (C_{H} vs. C_{C} and D_{H} vs.

D_{C}). Overall, these results suggest that corals hosting *Durusdinium* respond to thermal stress with substantially less and different methylation changes than those of *Cladocopium*-hosting corals.

Functional enrichment analysis of DMGs identified 34 overrepresented GO terms across significant DMGs in all contrasts (Table 2). However, GO_MWU analysis using all 1040 genes with methylation data available, did not find any GO significantly hypo- or hypermethylated for any of the treatment groups. Similarly, KOG_MWU analysis showed no significantly hypo- or hypermethylated category across contrasts (Figure S4A). KOG delta ranks (Figure S4B), however, were significantly correlated between the symbiont shuffling contrast (D_{C} vs. C_{C}) and the responses to heat stress of both, *Cladocopium*-dominated corals (C_{H} vs. C_{C} ; $R = -0.74$, CI 95% [-0.47, -0.89]) and *Durusdinium*-dominated corals (D_{H} vs. D_{C} ; $R = 0.61$, CI 95% [0.25, 0.81]) but in opposite directions. No correlation was observed between the heat stress responses of both symbionts.

FIGURE 4 Transposable elements methylation and expression by treatment combination (a) Density of methylated positions in repeat region types by treatment combination (b) Expression of repeat elements for each of the treatment combinations. Error bars denote 1 SE. DNA: DNA transposons; LINE: long interspersed nuclear elements; LTR: long terminal repeat; SINE: short interspersed nuclear elements; srpRNA: signal recognition particle RNA



Similarly to the case of individual genes, results from DMGs support that DNA methylation responses to heat stress are dependent on the dominant symbiont.

3.6 | Interaction between DNA methylation and gene expression

Using a gene expression data set previously produced for the same set of samples (Cunning & Baker, 2020), hypotheses were tested about the correlation between DNA methylation and gene expression. No linear correlation was observed between mean gene-body methylation and gene expression for control corals ($R^2 = 0.0019$, $p = .348$, Figure 5b). DNA methylation, however, did show a marginally significant (for $\alpha = 0.1$) negative correlation with gene expression CV ($R^2 = 0.0066$, $p = .0766$, Figure 5c), hinting a decrease in DNA methylation in genes with more variable expression. Finally, the association between the responses of DNA methylation and gene expression to the symbiont and temperature manipulations was also evaluated using linear regression (Figure S5). Again, no significant correlation was observed for any of the contrasts, neither for all covered genes nor for DMGs only, in correspondence with the lack of shared DMGs/DEGs (i.e., differentially expressed genes) found for all contrasts (Figure 5d). Overall, these results are consistent with a DNA methylation response to experimental manipulations, showing certain similarities to the transcriptome, although lacking evidence of a direct association between gene expression and DNA methylation at the gene level.

4 | DISCUSSION

This work constitutes the first evaluation of the epigenetic responses to symbiont manipulations in stony corals, and the first description of the DNA methylation landscape of the great star coral *M. cavernosa*, including its response to heat stress. The complementarity

between the data sets developed in this work and the transcriptional plasticity data developed by (Cunning & Baker, 2020), allowed the analysis of the interactions between gene expression and DNA methylation in response to symbiont manipulations and thermal stress. Differential DNA methylation in response to both symbiont and temperature manipulations was identified at single nucleotide, region, and gene levels, following a global pattern similar to that observed in the transcriptional response (Cunning & Baker, 2020). Both differentially methylated regions and genes (DMRs and DMGs) indicate a divergent response to heat stress for corals dominated by *Cladocodium* or *Durusdinum* symbionts. However, no clear evidence of direct interaction between gene body methylation (gbM) and expression was observed, and only inconclusive evidence supporting a role of DNA methylation in decreasing spurious transcription was found.

4.1 | The DNA methylation landscape of *M. cavernosa* depicts a relatively stress resistant coral

About 19% of all CpGs in the genome of *M. cavernosa* were methylated and primarily located in intergenic regions (>60% for all CpGs and methylated CpGs). This is comparable with the DNA methylation levels observed in other marine invertebrates (Gavery & Roberts, 2013; Strader et al., 2020; Venkataraman et al., 2020), including the relatively stress resistant corals *Porites astreoides* (Dimond & Roberts, 2020) and *Montipora capitata* (Trigg et al., 2021). Remarkably, methylation levels are significantly higher than those reported for the cnidarian model *Aiptasia* sp. (6.7%; [Li et al., 2018]), the stress-sensitive coral *Stylophora pistillata* (7%, [Liew et al., 2018]), and other corals of the robust clade like *Pocillopora acuta* (<10%; Trigg et al., 2021) and *Acropora cervicornis* (<10%; J. A. Rodriguez-Casariego, unpublished data).

Methylated CpGs observed in *M. cavernosa* significantly concentrate in introns and transposable elements (on both genic and

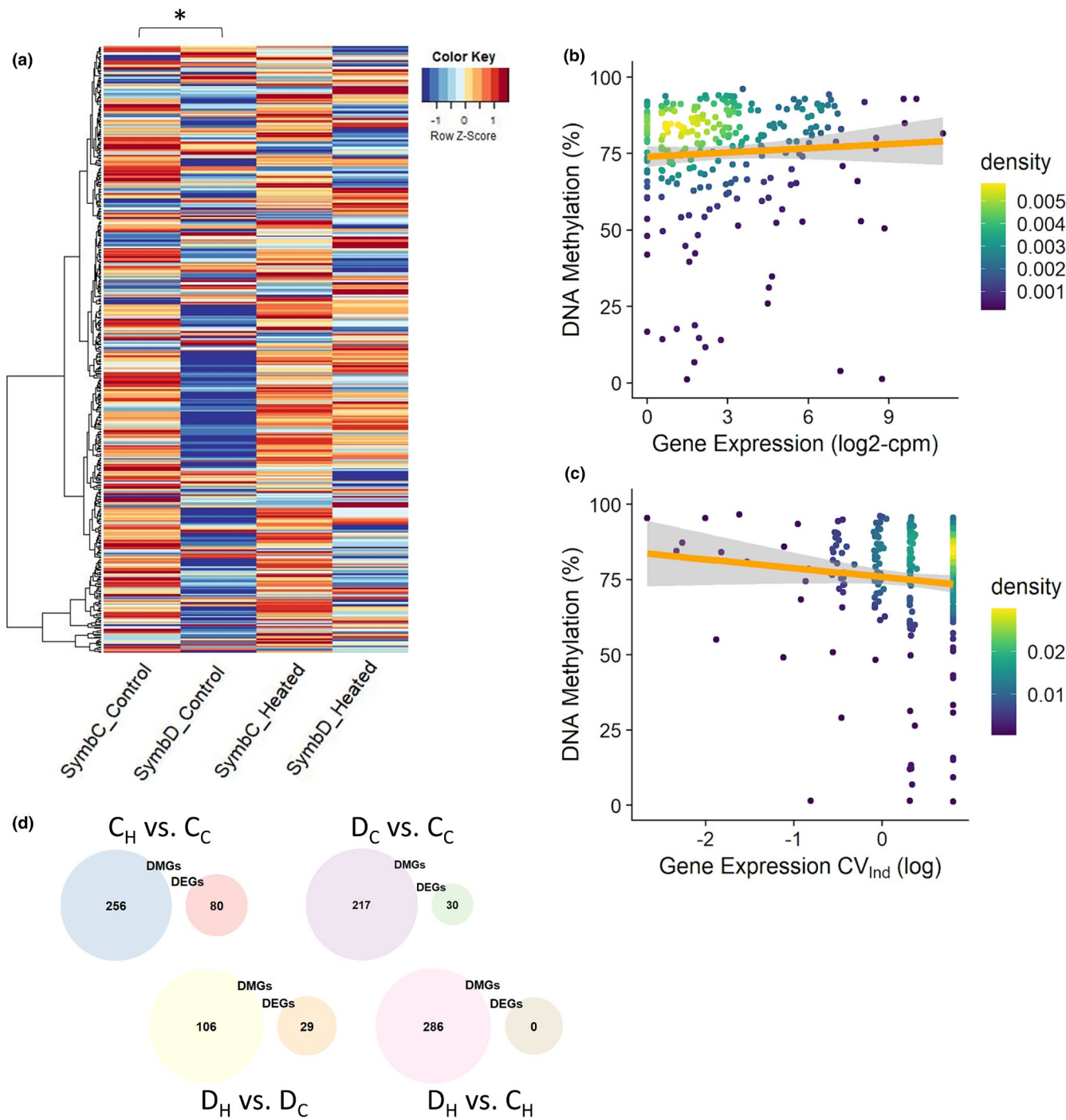


FIGURE 5 Differentially methylated genes (DMGs) and correlation with gene expression. (a) Heatmap representing methylation changes for all significant DMGs across all treatments. (*) represent significant differences ($p.\text{adj} = .0429$) in total gene body methylation mean evaluated through pairwise t test with Benjamini-Hochberg correction. (b) Represents the level of gene DNA methylation compared with gene expression CV across individuals in the control-*Cladocopium* group. DNA methylation was not significantly correlated with gene expression ($R^2 = 0.0053$, $p = .3265$), but it was marginally significantly correlated with gene expression CV_{Ind} ($R^2 = 0.0219$, $p < .0441$). Given the low coverage (Figure S2) no filter was applied and $n = 185$ genes were included. (c) Venn diagram comparing differentially methylated genes (DMG) and differentially expressed genes (DEG, data obtained from Cunningham & Baker, 2020) for each of the contrasts between experimental groups (Ch, *Cladocopium*/heated; Cc, *Cladocopium*/control; Dh, *Durusdinium*/heated; Dc, *Durusdinium*/control)

intergenic regions) when compared to the global distribution of CpGs in the genome. While gene-body methylation is characteristic of invertebrates (Feng et al., 2010; Gavery & Roberts, 2013), including corals (Dixon et al., 2018; Liew et al., 2018), the presence of similar

DNA methylation levels in intergenic regions and transposable elements represents a new evidence never observed before in corals. An increased DNA methylation of transposable elements has been previously observed in plants (Cantu et al., 2010), mammals (Jansz,

TABLE 2 Gene ontology (GO) categories overrepresented in differentially methylated genes (DMGs)

Contrast	Ontology	Genes	GO term	p.adj	
Cc. vs. Ch	BP	3/3	Endoplasmic reticulum to Golgi vesicle-mediated transport	.0178	
		4/6	Ion transport	.0327	
		4/6	Golgi organization	.0378	
		3/4	Autophagosome assembly	.0462	
		5/8	RNA-directed DNA polymerase activity	.0246	
	MF	3/4	ARF guanyl-nucleotide exchange factor activity	.0474	
		4/4	Positive regulation of I-kappaB kinase/NF-kappaB signaling	.0022	
		5/10	Apoptotic process	.0391	
		4/7	Actin cytoskeleton organization	.0430	
		2/2	Histone deacetylation	.0446	
Cc. vs. Dc	BP	2/2	Chemotaxis	.0493	
		2/2	Cellular response to testosterone stimulus	.0496	
		CC	11/21	Extracellular region	.0018
		CC	2/2	Retrotransposon nucleocapsid	.0364
		CC	2/2	Mitotic spindle pole	.0437
	MF	2/2	Spindle pole centrosome	.0496	
		3/4	RNA-DNA hybrid ribonuclease activity	.0348	
		2/2	Ribonuclease activity	.0364	
		2/2	Tumor necrosis factor receptor binding	.0415	
		BP	5/6	Golgi organization	.0089
Ch. vs. Dh	BP	5/8	G protein-coupled receptor signaling pathway	.0414	
		5/8	Negative regulation of apoptotic process	.0459	
		CC	12/23	Integral component of plasma membrane	.0086
		MF	4/5	Thiol-dependent ubiquitin-specific protease activity	.0178
		MF	4/5	Cysteine-type endopeptidase activity	.0270
	MF	4/5	Microtubule motor activity	.0314	
		BP	2/2	Regulation of protein localization	.0092
		BP	2/3	Cerebellar Purkinje cell differentiation	.0371
		BP	2/3	Negative regulation of autophagy	.0418
		BP	2/4	Positive regulation of angiogenesis	.0472
Dc. vs. Dh	BP	CC	8/23	Integral component of plasma membrane	.0011
		CC	2/2	cell projection	.0175
		MF	2/2	Kinesin binding	.0122
	MF	MF	3/8	RNA-directed DNA polymerase activity	.0375

Note: p.adj: Benjamini-Hochberg adjusted p.value.

2019) and other invertebrates (Venkataraman et al., 2020), and has been attributed to the defence role of DNA methylation by selectively inhibiting mobile elements in the genome (Choi et al., 2020). It thus may be plausible that, also in the case of corals, DNA methylation participates in the regulation of mobile element activity in the genome, potentially generating new genetic combinations. Lastly, Exons displayed higher methylation levels and lower methylation variability than introns and intergenic regions. This aligns with DNA

methylation patterns observed in other invertebrates (Downey-Wall et al., 2020; Lyko et al., 2010), and could be related with a role of this epigenetic mechanism in the regulation of differential splicing (Flores et al., 2012; Lyko et al., 2010). Nonetheless, since other studies have described higher DNA methylation levels in the introns of the coral *S. pistillata* (Liew et al., 2018), further studies will be required in order to fully elucidate the linkages between DNA methylation and genome architecture.

4.2 | Symbiont manipulation and thermal stress produce distinctive DNA methylation responses

Symbiont manipulation and thermal stress triggered particular environmentally responsive changes in the methylome of *M. cavernosa*, suggesting the existence of distinctive responses for the different types of manipulations used in the present study. Estimates of global DNA methylation levels, however, failed to detect differences between treatment groups, consistent with previous reports suggesting that this approach provides a poor descriptor of environmental responsiveness in corals (i.e., “seesaw” patterns with increases and decreases in DNA methylation cancelling each other to produce invariant values (Dimond & Roberts, 2020; Dixon et al., 2018]). This is further supported by the identification of DMRs and DMGs between symbiont compositions and thermal treatments reported in the present work, suggesting significant differences in DNA methylation.

The present work evidences a genet- and treatment-specific DNA methylation response that is influenced by the coral genotype, in agreement with previous studies in other scleractinian species (Durante et al., 2019; Liew et al., 2018; Rodríguez-Casariego et al., 2020). In this case, genets also responded differently to symbiont and temperature manipulations. However, across all genets, a clear treatment-specific response and symbiont-driven heat stress pattern was indicated by ordination analyses and variance partitioning. Given that symbiont shuffling was achieved by thermal bleaching, there is a possibility that the observed differences between symbionts are due to that previous bleaching and not the effect of the symbiont identity. In their study, Cunning and Baker (2020) discarded such carry-over effects by analysing the transcriptome of corals that bleached and recovered with the native symbiont before being subject to heat-stress. Since that analysis was not possible in the present work, the contribution of DNA methylation changes maintained through epigenetic memory cannot be fully neglected. Overall, shifts in symbiont dominance from *Cladocopium* to *Durusdinium* appear to drive DNA methylation changes influencing subsequent responses to thermal stress, in agreement with the transcriptomic (Cunning & Baker, 2020) and phenotypic features (i.e., thermal resistance) conferred to corals by this shift (Silverstein et al., 2015).

4.2.1 | Gene body DNA methylation does not correlate with gene expression

Epigenetic modifications play a central role in phenotypic plasticity during environmental responses (Eirin-Lopez & Putnam, 2019). However, the underpinnings of how epigenetic mechanisms convey environmental signals to the genome and the resulting shaping of its function is still uncertain, especially in the case of non-model organisms (Eirin-Lopez & Putnam, 2019). Accordingly, invertebrate genomes are significantly less methylated than vertebrate genomes, with DNA methylation accumulating in gene bodies in the former as opposed to promoters in the latter (Dixon et al., 2016; Gavery & Roberts, 2013). Such differences have generated multiple hypotheses describing the role of gene body methylation regulating gene

expression (Duncan et al., 2014). In cnidarians, the hypothesis most widely supported is the reduction of spurious transcription through the blocking of intragenomic initiation positions (Dixon et al., 2018; Li et al., 2018; Liew et al., 2018; Roberts & Gavery, 2012). The results obtained in the present work provide additional support to this hypothesis, based on the higher levels of methylation detected in *M. cavernosa* genes displaying less variable transcription. However, the links between differentially methylated genes and changes in gene expression remained elusive, with significant changes in gene-body methylation occurring in genes with no differential expression regardless of the similarities of the global responses of both mechanisms to the experimental manipulations. Similar results were observed before in corals (Liew et al., 2018) and other cnidarians (Li et al., 2018), with very scarce overlapping between differentially methylated and expressed genes.

Interestingly, the widely observed positive correlation between gene body DNA methylation and gene expression levels in corals (Dixon et al., 2018; Liew et al., 2018) was not evidenced here. MBD-BS bias towards methylated fragments could reduce the number of genes covered by this method (Trigg et al., 2021), especially in species with higher methylation levels such as *Montipora capitata* (Trigg et al., 2021) or *M. cavernosa* as evidenced here. Therefore, a limited representation of lowly methylated genes (potentially inducible genes; Dixon et al., 2018), could have influenced our results.

The present study found a significant accumulation of DMRs in transposable elements (TEs, including repetitive regions), consistent with the proposed role of DNA methylation mediating TE transcriptional silencing (Choi et al., 2020; Feschotte et al., 2002). Remarkably, the expression of LTRs (retrotransposons linked to transcriptional regulation in plants [Jia et al., 2014]), was significantly different between thermal treatments regardless of the dominant symbiont. Based on these results, it is tempting to hypothesize a link between DNA methylation and the regulation of repetitive regions, constituting a very attractive direction for future analyses.

4.3 | Conclusions

The present work provides evidence suggesting that DNA methylation plays an important role mediating the interaction between holobiont composition and phenotypic responses in the coral *M. cavernosa*. Importantly, such a role does not seem to involve a direct influence (at least necessarily) on gene expression regulation. Both symbiont manipulation and heat stress elicited DNA methylation responses that were not homogeneous across genotypes, but consistently showed a treatment-specific pattern. DNA methylation response to heat stress was dependent on the dominant symbiont, with twice as many significant DMRs found between heated corals hosting different symbionts (D_H vs. C_H contrast). Similarly to the transcriptional response of *M. cavernosa* to these manipulations (Cunning & Baker, 2020), *Durusdinium*-dominated corals displayed a potentially “milder” DNA methylation response to thermal stress. On the other hand, no evidence of a direct association between gene

expression and DNA methylation at the gene level was found, other than the previously described reduction of transcriptional variability on highly methylated genes (Li et al., 2018; Liew et al., 2018). Remarkably, our analyses showed significant accumulation of methylated and differentially methylated loci in transposable elements. Given the activation of some of these elements in response to heat stress, the obtained results could provide new research avenues to link DNA methylation with transcriptional and phenotypic plasticity involving the regulation of repetitive regions in the genome.

ACKNOWLEDGEMENTS

This work was supported by grants from the National Science Foundation (1921402) and from the National Oceanic and Atmospheric Administration (NA21NMF4820301) awarded to J.E.-L., and a grant from the National Science Foundation (1547798) awarded to Florida International University as part of the Centres for Research Excellence in Science and Technology Program. J.A.R.C. was supported by awards from FIU Tropics and AMLC. A.C.B and R.C. were supported by Mote "Protect Our Reefs" License Plate Grant (POR2016-15). Corals were collected under permit SAL-17-1182-SRP. We are thankful to Dr Steven Roberts and his laboratory members for assistance with MBD-BS library preparation and analysis. Thanks are also due to Dr Mikhail Matz for providing access to the *M. cavernosa* genome assembly. This is contribution number 290 from the Coastlines and Oceans Division of the Institute of Environment at Florida International University.

DATA AVAILABILITY STATEMENT

Raw sequence data has been made available at the NCBI Sequence Read Archive under accession number PRJNA750791. Pipelines details, code and processed data sets can be found at github.com/jarcasariego/MCAV_methylation and archived at Zenodo as (Rodriguez-Casariego, 2021: <https://doi.org/10.5281/zenodo.5348322>).

ORCID

Javier A. Rodriguez-Casariego  <https://orcid.org/0000-0001-9955-4721>

Ross Cunning  <https://orcid.org/0000-0001-7241-1181>

Jose M. Eirin-Lopez  <https://orcid.org/0000-0002-8041-9770>

REFERENCES

Alexa, A., Rahnenführer, J., & Lengauer, T. (2006). Improved scoring of functional groups from gene expression data by decorrelating GO graph structure. *Bioinformatics*, 22(13), 1600–1607. <https://doi.org/10.1093/bioinformatics/btl140>

Baker, A. C. (2004). Symbiont diversity on coral reefs and its relationship to bleaching resistance and resilience. *Coral Health and Disease*. https://doi.org/10.1007/978-3-662-06414-6_8

Baker, A. C., & Cunning, R. (2015). Coral 'bleaching' as a generalized stress response to environmental disturbance. *Diseases of Coral*, 396–409.

Barfield, S. J., Aglyamova, G. V., Bay, L. K., & Matz, M. V. (2018). Contrasting effects of symbiodinium identity on coral host transcriptional profiles across latitudes. *Molecular Ecology*, 27(15), 3103–3115.

Barshis, D. J. (2015). Genomic potential for coral survival of climate change. *Coral Reefs in the Anthropocene*, https://doi.org/10.1007/978-94-017-7249-5_7

Bay, L. K., Rocker, M., Boström-Einarsson, L., Babcock, R., Buerger, P., Cleves, P., Harrison, D., Negri, A., Quigley, K., Randall, C. J., & van Oppen, M. J. (2019). Reef restoration and adaptation program: intervention technical summary. a report provided to the australian government by the reef restoration and adaptation program. *Reef Restoration and Adaptation Program*.

Berkelmans, R., & van Oppen, M. J. H. (2006). The role of zooanthellae in the thermal tolerance of corals: a 'nugget of hope' for coral reefs in an era of climate change. *Proceedings of the Royal Society B: Biological Sciences*, 273(1599), 2305–2312. <https://doi.org/10.1098/rspb.2006.3567>

Cantu, D., Vanzetti, L. S., Sumner, A., Dubcovsky, M., Matvienko, M., Distelfeld, A., Michelmore, R. W., & Dubcovsky, J. (2010). Small RNAs, DNA methylation and transposable elements in wheat. *BMC Genomics*, 11(June), 408.

Cavalli, G., & Heard, E. (2019). Advances in epigenetics link genetics to the environment and disease. *Nature*, 571(7766), 489–499. <https://doi.org/10.1038/s41586-019-1411-0>

Choi, J., Lyons, D. B., Yvonne Kim, M., Moore, J. D., & Zilberman, D. (2020). DNA methylation and histone H1 jointly repress transposable elements and aberrant intragenic transcripts. *Molecular Cell*, 77(2), 310–23.e7. <https://doi.org/10.1016/j.molcel.2019.10.011>

Cunning, R., & Baker, A. C. (2013). Excess algal symbionts increase the susceptibility of reef corals to bleaching. *Nature Climate Change*, 3(3), 259–262. <https://doi.org/10.1038/nclimate1711>

Cunning, R., & Baker, A. C. (2020). Thermotolerant coral symbionts modulate heat stress-responsive genes in their hosts. *Molecular Ecology*, 29(15), 2940–2950. <https://doi.org/10.1111/mec.15526>

DeSalvo, M. K., Sunagawa, S., Fisher, P. L., Voolstra, C. R., Iglesias-Prieto, R., & Medina, M. (2010). Coral host transcriptomic states are correlated with symbiodinium genotypes. *Molecular Ecology*, 19(6), 1174–1186.

Dimond, J. L., Gamblewood, S. K., & Roberts, S. B. (2017). Genetic and epigenetic insight into morphospecies in a reef coral. *Molecular Ecology*, 26(19), 5031–5042.

Dimond, J. L., & Roberts, S. B. (2020). Convergence of DNA methylation profiles of the reef coral *porites astreoides* in a novel environment. *Frontiers in Marine Science*, 6, 792. <https://doi.org/10.3389/fmars.2019.000792>

Dixon, G. B., Bay, L. K., & Matz, M. V. (2016). Evolutionary consequences of DNA methylation in a basal metazoan. *Molecular Biology and Evolution*, 33(9), 2285–2293. <https://doi.org/10.1093/molbev/msw100>

Dixon, G., Liao, Y. I., Bay, L. K., & Matz, M. V. (2018). Role of gene body methylation in acclimatization and adaptation in a basal metazoan. *Proceedings of the National Academy of Sciences of the United States of America*, 115(52), 13342–13346. <https://doi.org/10.1073/pnas.1813749115>

Downey-Wall, A. M., Cameron, L. P., Ford, B. M., McNally, E. M., Venkataraman, Y. R., Roberts, S. B., Ries, J. B., & Lotterhos, K. E. (2020). Ocean acidification induces subtle shifts in gene expression and DNA methylation in mantle tissue of the Eastern Oyster (*Crassostrea virginica*). *Frontiers in Marine Science*, 7, 828. <https://doi.org/10.3389/fmars.2020.566419>

Duncan, E. J., Gluckman, P. D., & Dearden, P. K. (2014). Epigenetics, plasticity, and evolution: how do we link epigenetic change to phenotype? *Journal of Experimental Zoology Part B, Molecular and Developmental Evolution*, 322(4), 208–220. <https://doi.org/10.1002/jez.b.22571>

Durante, M. K., Baums, I. B., Williams, D. E., Vohsen, S., & Kemp, D. W. (2019). what drives phenotypic divergence among coral clonemates of *acropora palmata*? *Molecular Ecology*, 28(13), 3208–3224.

Eirin-Lopez, J. M., & Putnam, H. M. (2019). Marine environmental epigenetics. *Annual Review of Marine Science*, 11(1), 335–368. <https://doi.org/10.1146/annurev-marine-010318-095114>

Feng, S., Cokus, S. J., Zhang, X., Chen, P.-Y., Bostick, M., Goll, M. G., Hetzel, J., Jain, J., Strauss, S. H., Halpern, M. E., Ukomadu, C., Sadler, K. C., Pradhan, S., Pellegrini, M., & Jacobsen, S. E. (2010). Conservation and divergence of methylation patterning in plants and animals. *Proceedings of the National Academy of Sciences of the United States of America*, 107(19), 8689–8694. <https://doi.org/10.1073/pnas.1002720107>

Feschotte, C., Jiang, N., & Wessler, S. R. (2002). Plant transposable elements: Where genetics meets genomics. *Nature Reviews Genetics*, 3(5), 329–341.

Flores, K., Wolschin, F., Corneveaux, J. J., Allen, A. N., Huentelman, M. J., & Amdam, G. V. (2012). Genome-Wide Association between DNA Methylation and Alternative Splicing in an Invertebrate. *BMC Genomics*, 13(September), 480. <https://doi.org/10.1186/1471-2164-13-480>

Gavery, M. R., & Roberts, S. B. (2013). Predominant intragenic methylation is associated with gene expression characteristics in a bivalve mollusc. *PeerJ*, 1(November), e215. <https://doi.org/10.7717/peerj.215>

Glynn, P. W., Maté, J. L., Baker, A. C., & Calderón, M. O. (2001). Coral bleaching and mortality in panama and ecuador during the 1997–1998 El Niño-Southern oscillation event: Spatial/temporal patterns and comparisons with the 1982–1983 event. *Bulletin of Marine Science*, 69(1), 79–109.

Helmkampf, M., Renee Bellinger, M., Frazier, M., & Takabayashi, M. (2019). Symbiont type and environmental factors affect transcriptome-wide gene expression in the coral *montipora capitata*. *Ecology and Evolution*, 9(1), 378–392.

Hoffman, G. E., & Schadt, E. E. (2016). variancePartition: Interpreting drivers of variation in complex gene expression studies. *BMC Bioinformatics*, 17(1), 483. <https://doi.org/10.1186/s12859-016-1323-z>

Hughes, T. P., Kerry, J. T., Álvarez-Noriega, M., Álvarez-Romero, J. G., Anderson, K. D., Baird, A. H., Babcock, R. C., Beger, M., Bellwood, D. R., Berkelmans, R., Bridge, T. C., Butler, I. R., Byrne, M., Cantin, N. E., Comeau, S., Connolly, S. R., Cumming, G. S., Dalton, S. J., Diaz-Pulido, G., ... Wilson, S. K. (2017). Global warming and recurrent mass bleaching of corals. *Nature*, 543(7645), 373–377. <https://doi.org/10.1038/nature21707>

Jansz, N. (2019). DNA methylation dynamics at transposable elements in mammals. *Essays in Biochemistry*, 63(6), 677–689. <https://doi.org/10.1042/EBC20190039>

Jia, L. I., Lou, Q., Jiang, B., Wang, D., & Chen, J. (2014). LTR retrotransposons cause expression changes of adjacent genes in early generations of the newly formed allotetraploid *cucumis hystivus*. *Scientia Horticulturae*, 174, 171–177. <https://doi.org/10.1016/j.scienta.2014.05.022>

Jombart, T., Devillard, S., & Balloux, F. (2010). Discriminant analysis of principal components: A new method for the analysis of genetically structured populations. *BMC Genetics*, 11(October), 94. <https://doi.org/10.1186/1471-2156-11-94>

Jones, A., Berkelmans, R., van Oppen, M. J. H., Mieog, J. C., & Sinclair, W. (2008). A Community change in the algal endosymbionts of a scleractinian coral following a natural bleaching event: Field evidence of acclimatization. *Proceedings of the Royal Society B: Biological Sciences*, 275(1641), 1359–1365.

Kim, D., Langmead, B., & Salzberg, S. L. (2015). hisat2. *Nature Methods*, 944.

Krueger, F. (2012). Trim Galore: A Wrapper Tool around Cutadapt and FastQC to Consistently Apply Quality and Adapter Trimming to FastQ Files, with Some Extra Functionality for Mspl-Digested RRBS-Type (Reduced Representation Bisulfite-Seq) Libraries. http://www.Bioinformatics.Babraham.Ac.Uk/projects/trim_galore/ (Date of Access: 28/04/2016).

Krueger, F., & Andrews, S. R. (2011). Bismark: a flexible aligner and methylation caller for Bisulfite-Seq applications. *Bioinformatics*, 27(11), 1571–1572.

Langmead, B., & Salzberg, S. L. (2012). Fast gapped-read alignment with Bowtie 2. *Nature methods*, 9(4), 357–359.

Li, H., Handsaker, B., Wysoker, A., Fennell, T., Ruan, J., Homer, N., Marth, G., Abecasis, G., & Durbin, R.; 1000 Genome Project Data Processing Subgroup. (2009). The sequence alignment/map format and SAMtools. *Bioinformatics*, 25(16), 2078–2079. <https://doi.org/10.1093/bioinformatics/btp352>

Li, Y., Liew, Y. J., Cui, G., Cziesielski, M. J., Zahran, N., Michell, C. T., Voolstra, C. R., & Aranda, M. (2018). DNA methylation regulates transcriptional homeostasis of algal endosymbiosis in the coral model *aiptasia*. *Science Advances*, 4(8), eaat2142. <https://doi.org/10.1126/sciadv.aat2142>

Liew, Y. J., Howells, E. J., Wang, X., Michell, C. T., Burt, J. A., Idaghdour, Y., & Aranda, M. (2020). Intergenerational epigenetic inheritance in reef-building corals. *Nature Climate Change*, 10(3), 254–259.

Liew, Y. J., Zoccola, D., Li, Y., Tambutté, E., Venn, A. A., Michell, C. T., Cui, G., Deutekom, E. S., Kaandorp, J. A., Voolstra, C. R., Forêt, S., Allemand, D., Tambutté, S., & Aranda, M. (2018). Epigenome-associated phenotypic acclimatization to ocean acidification in a reef-building coral. *Science Advances*, 4(6), eaar8028.

Lyko, F., Foret, S., Kucharski, R., Wolf, S., Falckenhayn, C., & Maleszka, R. (2010). The honey bee epigenomes: Differential methylation of brain DNA in queens and workers. *PLoS Biology*, 8(11), e1000506. <https://doi.org/10.1371/journal.pbio.1000506>

Matz, M. V. (2016). KOGMWU: Functional summary and meta-analysis of gene expression data. *R Package Version 1*.

National Academies of Sciences, Engineering, and Medicine, Division on Earth and Life Studies, Board on Life Sciences, Ocean Studies Board, and Committee on Interventions to Increase the Resilience of Coral Reefs. (2019). *A research review of interventions to increase the persistence and resilience of coral reefs*. National Academies Press.

Pandolfi, J. M., Bradbury, R. H., Sala, E., Hughes, T. P., Bjoerndal, K. A., Cooke, R. G., McArdle, D., McClenaghan, L., Newman, M. J. H., Paredes, G., Warner, R. R., & Jackson, J. B. C. (2003). Global trajectories of the long-term decline of coral reef ecosystems. *Science*, 301(5635), 955–958. <https://doi.org/10.1126/science.1085706>

Pettay, D. T., Wham, D. C., Smith, R. T., Iglesias-Prieto, R., & LaJeunesse, T. C. (2015). Microbial invasion of the caribbean by an Indo-Pacific Coral Zooxanthella. *Proceedings of the National Academy of Sciences of the United States of America*, 112(24), 7513–7518. <https://doi.org/10.1073/pnas.1502283112>

Prada, C., Hanna, B., Budd, A. F., Woodley, C. M., Schmutz, J., Grimwood, J., Iglesias-Prieto, R., Pandolfi, J. M., Levitan, D., Johnson, K. G., Knowlton, N., Kitano, H., DeGiorgio, M., & Medina, M. (2016). Empty Niches after Extinctions Increase Population Sizes of Modern Corals. *Current biology : CB*, 26(23), 3190–3194. <https://doi.org/10.1016/j.cub.2016.09.039>

Putnam, H. M., Davidson, J. M., & Gates, R. D. (2016). Ocean acidification influences host DNA methylation and phenotypic plasticity in environmentally susceptible corals. *Evolutionary Applications*, <https://doi.org/10.1111/eva.12408>

Quigley, K. M., Baker, A. C., Coffroth, M. A., Willis, B. L., & van Oppen, M. J. H. (2018). Bleaching resistance and the role of algal endosymbionts. *Ecological Studies*, https://doi.org/10.1007/978-3-319-75393-5_6

Quinlan, A. R., & Hall, I. M. (2010). BEDTools: a flexible suite of utilities for comparing genomic features. *Bioinformatics*, 26(6), 841–842. <https://doi.org/10.1093/bioinformatics/btq033>

R Core Team (2020). *R: A language and environment for statistical computing*. Vienna, Austria: R Foundation for Statistical Computing. <https://www.R-project.org/>

Rivera-Casas, C., Gonzalez-Romero, R., Garduño, R. A., Cheema, M. S., Ausio, J., & Eirin-Lopez, J. M. (2017). Molecular and biochemical methods useful for the epigenetic characterization of chromatin-associated proteins in bivalve molluscs. *Frontiers in physiology*, 8, 490.

Roberts, S. B., & Gavery, M. R. (2012). Is There a relationship between DNA methylation and phenotypic plasticity in invertebrates? *Frontiers in Physiology*, 2, <https://doi.org/10.3389/fphys.2011.00116>

Rodríguez-Casariego, J. A., Ladd, M. C., Shantz, A. A., Lopes, C., Cheema, M. S., Kim, B., Roberts, S. B., Fourqurean, J. W., Ausio, J., Burkepile, D. E., & Eirin-Lopez J. M. (2018). Coral epigenetic responses to nutrient stress: Histone H2A.X phosphorylation dynamics and DNA methylation in the staghorn coral *Acropora cervicornis*: XXXX. *Ecology and Evolution*, 8(23), 12193–12207.

Rodríguez-Casariego, J. A., Mercado-Molina, A. E., García-Souto, D., Ortiz-Rivera, I. M., Lopes, C., Baums, I. B., Sabat, A. M., & Eirin-Lopez, J. M. (2020). Genome-wide DNA methylation analysis reveals a conserved epigenetic response to seasonal environmental variation in the staghorn coral *Acropora cervicornis*. *Frontiers in Marine Science*, 7, 822. <https://doi.org/10.3389/fmars.2020.560424>

R Studio Team (2020). *RStudio: Integrated Development for R*. PBC, Boston, MA: RStudio. <http://www.rstudio.com/>

Schultz, M. D., He, Y., Whitaker, J. W., Hariharan, M., Mukamel, E. A., Leung, D., Rajagopal, N., Nery, J. R., Urich, M. A., Chen, H., Lin, S., Lin, Y., Jung, I., Schmitt, A. D., Selvaraj, S., Ren, B., Sejnowski, T. J., Wang, W., & Ecker, J. R. (2015). Human body epigenome maps reveal noncanonical DNA methylation variation. *Nature*, 523(7559), 212–216. <https://doi.org/10.1038/nature14465>

Shinzato, C., Khalturin, K., Inoue, J., Zayasu, Y., Kanda, M., Kawamitsu, M., Yoshioka, Y., Yamashita, H., Suzuki, G., & Satoh, N. (2021). Eighteen Coral Genomes Reveal the Evolutionary Origin of *Acropora* Strategies to Accommodate Environmental Changes. *Molecular biology and evolution*, 38(1), 16–30. <https://doi.org/10.1093/molbev/msaa216>

Shinzato, C., Shoguchi, E., Kawashima, T., Hamada, M., Hisata, K., Tanaka, M., Fujie, M., Fujiwara, M., Koyanagi, R., Ikuta, T., Fujiyama, A., Miller, D. J., & Satoh, N. (2011). Using the *Acropora digitifera* genome to understand coral responses to environmental change. *Nature*, 476(7360), 320–323. <https://doi.org/10.1038/nature10249>

Silverstein, R. N., Cunning, R., & Baker, A. C. (2015). Change in algal symbiont communities after bleaching, not prior heat exposure, increases heat tolerance of reef corals. *Global Change Biology*, 21(1), 236–249. <https://doi.org/10.1111/gcb.12706>

Strader, M. E., Kozal, L. C., & Leach, T. S. (2020). Examining the role of DNA methylation in transcriptomic plasticity of early stage sea urchins: Developmental and maternal effects in a kelp forest herbivore. *Frontiers in Marine*. <https://pdfs.semanticscholar.org/ad25/b781263b271bc905a3621f7aa1b427bb58a5.pdf>

Swain, T. D., Lax, S., Backman, V., & Marcelino, L. A. (2020). Uncovering the role of symbiodiniaceae assemblage composition and abundance in coral bleaching response by minimizing sampling and evolutionary biases. *BMC Microbiology*, 20(1), 124. <https://doi.org/10.1186/s12866-020-01765-z>

Trigg, S. A., Venkataraman, Y. R., Gavery, M., Roberts, S. B. (2021). Invertebrate methylomes provide insight into mechanisms of environmental tolerance and reveal methodological biases. *BioRxiv*. <https://www.biorxiv.org/content/10.1101/2021.03.29.437539v1>. abstract

Venkataraman, Y. R., Downey-Wall, A. M., Ries, J., Westfield, I., White, S. J., Roberts, S. B., & Lotterhos, K. E. (2020). General DNA methylation patterns and environmentally-induced differential methylation in the Eastern Oyster (*Crassostrea virginica*). *Frontiers in Marine Science*, 7, 225. <https://doi.org/10.3389/fmars.2020.00225>

Voolstra, C. R., Li, Y., Liew, Y. J., Baumgarten, S., Zoccola, D., Flot, J. F., Tambutté, S., Allemand, D., & Aranda, M. (2017). Comparative analysis of the genomes of *Stylophora pistillata* and *Acropora digitifera* provides evidence for extensive differences between species of corals. *Scientific reports*, 7(1), 1–14.

Weis, V. M. (2008). Cellular mechanisms of cnidian bleaching: Stress causes the collapse of symbiosis. *The Journal of Experimental Biology*, 211(Pt 19), 3059–3066. <https://doi.org/10.1242/jeb.009597>

Wright, R. M., Aglyamova, G. V., Meyer, E., & Matz, M. V. (2015). Gene expression associated with white syndromes in a reef building coral, *Acropora hyacinthus*. *BMC Genomics*, 16(May), 371.

Yuyama, I., Ishikawa, M., Nozawa, M., Yoshida, M.-A., & Ikeo, K. (2018). Transcriptomic changes with increasing algal symbiont reveal the detailed process underlying establishment of coral-algal symbiosis. *Scientific Reports*, 8(1), 16802. <https://doi.org/10.1038/s41598-018-34575-5>

SUPPORTING INFORMATION

Additional supporting information may be found in the online version of the article at the publisher's website.

How to cite this article: Rodriguez-Casariego, J. A., Cunning, R., Baker, A. C., & Eirin-Lopez, J. M. (2021). Symbiont shuffling induces differential DNA methylation responses to thermal stress in the coral *Montastraea cavernosa*. *Molecular Ecology*, 00, 1–15. <https://doi.org/10.1111/mec.16246>